Scanning Microscopy

Volume 5 | Number 3 Article 2

8-21-1991

Digitized Cathodoluminescence Imaging of Minerals

Ian M. Steele
The University of Chicago

Follow this and additional works at: https://digitalcommons.usu.edu/microscopy

 Part of the Biology Commons

Recommended Citation

Steele, Ian M. (1991) "Digitized Cathodoluminescence Imaging of Minerals," *Scanning Microscopy*: Vol. 5 : No. 3 , Article 2.
Available at: https://digitalcommons.usu.edu/microscopy/vol5/iss3/2

This Article is brought to you for free and open access by the Western Dairy Center at DigitalCommons@USU. It has been accepted for inclusion in Scanning Microscopy by an authorized administrator of DigitalCommons@USU. For more information, please contact digitalcommons@usu.edu.

Scanning Microscopy, Vol. 5, No. 3, 1991 (Pages 611-618)
Scanning Microscopy International, Chicago (AMF O'Hare), IL 60666 USA

0891-7035/91$3.00+.00

DIGITIZED CATHODOLUMINESCENCE IMAGING OF MINERALS

Ian M. Steele

Department of Geophysical Sciences
The University of Chicago
5734 S. Ellis Ave.
Chicago, IL 60637
Phone No. (312)-702-8109

(Received for publication May 13, 1991, and in revised form August 21, 1991)

Abstract

Digital imaging with cathodoluminescence (CL) capability, provides an additional, quantitative imaging perspective. While CL images can be useful by themselves, most microbeam instruments allow simultaneous acquisition of other signals including backscattered electron (BSE), secondary electron (SE), and X-ray images providing a powerful set of data for interpretation. Digital panchromatic images allow the use of standard and advanced image processing now available on laboratory computers to enhance single images or provide a means of combining information from two or more images. Other advantages of digital CL images include: 1) selective scan rates to avoid image distortion; 2) adjustable dwell times at any point to collect sufficient light due to weak CL; 3) calibrated image scales allowing relocation of features for additional study.

Many minerals and synthetic phases show CL and these images often reveal textures either difficult or impossible to observe with other signals. Examples of digital CL images are presented for: 1) diamond, where complex internal textures are revealed including the presence of features possibly corresponding to giant platelets; 2) forsterite from the Allende meteorite where CL reveals complex zoning within single grains the intensity of which correlates with the Al and Ti; 3) terrestrial carbonate showing intricate banding, the intensity of which can be compared with X-ray images; 4) meteoritic melilite where the CL reveals complex zoning and intensity variation within minor included spinel phases.

Key words: Imaging, cathodoluminescence, diamond, olivine, carbonate, electron microprobe, minerals, image processing

Introduction

Historically, cathodoluminescence (CL) of minerals has been recorded on color film forming a permanent record. Although images are often spectacular, quantitative interpretation is limited mainly to visual description of colors and textures. For quantitative interpretation, one would like to know the composition changes which produce or correlate with different CL colors and intensities; one would also like to record spectral data and study their dependence on composition. Microbeam instruments including the scanning electron microscope (SEM) and electron microprobe (EMP) can extend the study of CL by collection and display of CL light to form a scanning CL image. This panchromatic CL intensity as detected by a photomultiplier can modulate a cathode ray tube (CRT) to produce a visual image representing the CL intensity distribution much like other SEM images. Spectral information is lost although photomultiplier tubes may be selected which are more sensitive to a specific spectral range. For frame scanning of several minutes, the light level may be too low to allow acceptable recorded images and the long decay time of some CL may preclude obtaining sharp images. To circumvent some of these problems, digital images can be obtained where the beam dwell time can be extended both to collect sufficient signal at low light levels and to allow CL decay from previous beam positions. These digital images can then be stored and later processed to increase contrast, reduce background, or otherwise extract specific information. With modern instrumentation, these digital CL images can be complemented by X-ray, backscattered electron, secondary electron, and absorbed current images. A comparison of the relative merits of film recording versus digital recording of CL is given by Steele (1990) while an excellent overview of CL instrumentation and use of CL as applied to geologic studies is given by Marshall (1988).

Equipment description and technique

Digital CL images have been obtained in a CAMECA SX-50 electron microprobe which has the

additional advantage of obtaining up to 4 X-ray images using wavelength dispersive detectors and an additional video signal, usually a BSE image. Routine image collection is controlled by the manufacturer's software and provides the following options.

1) Either stage scanning with a fixed beam or beam scanning with a fixed stage. The choice is partly dependent on the size of the area to be scanned with beam scanning limited to areas smaller than about 500 microns diameter because of loss of light collection efficiency. Stage scanning is used for mm to cm sized areas. If stage scanning is used with areas smaller than about 100 microns, the resulting images show the effect of stage reproducibility errors of ± 1 micron by a loss of resolution in the final image. While beam scanning is incremental, stage scanning is continuous producing additional loss of resolution in the final image due to slight mixing of contrasting boundaries.

2) Selected dwell time at each point to compensate for light intensity or to allow more counts from each X-ray channel.

3) Choice of step size in conjunction with the array dimensions to optimize the resolution of the image with the features to be seen. Array dimensions may include any combination of 64, 128, 256, 512, and 1024 pixels to give either square or rectangular images. A minimum step size for stage scanning is 1 micron, while the step size in beam scanning can be smaller and image rotation is possible.

For special applications, software has also been written to allow spectrometer adjustments at each point enabling more than 4 X-ray intensities to be obtained and integration times of up to minutes at any one point. Resulting images are limited in sampling density, but coarse variations in two dimensions are possible for minor elements in addition to CL. These images are especially useful for determining effects of minor or trace elements on the CL intensity.

The CL light is collected by Cassegrain optics and viewed through a port normally used for binocular observation of the sample. A photomultiplier housing replaces the binocular microscope and the CL light is incident on the photocathode. The type of multiplier tube can be selected to increase sensitivity in certain spectral regions based on the response of the photocathode material. Between the sample and the multiplier, the light undergoes four reflections and passes through a quartz vacuum window. Because the mirrors are Al coated, there is a 10% broad absorption at about 800 nm for each reflection giving a loss in sensitivity in the red and infra-red regions; this could be avoided by using silver coated mirrors. The output of the photomultiplier can be displayed on the standard viewing console for rapid recognition of CL features but the image frequently suffers from the scan rate being fast relative to the decay time of the CL. These samples which have persistent CL produce poor images with CL emitting areas stretched out in the scanning direction. The dwell time per pixel for a CL image is usually 1 to 10 milliseconds but longer times, usually 100 milliseconds, are used both to increase the CL signal to noise ratio and to allow simultaneous acquisition of X-ray intensities. Thus a 256 x 256 image requires about 2 hours for both CL and X-ray image acquisition.

The two dimensional digital CL intensity data can be accepted by standard image processing programs. To allow simultaneous data collection and data analysis, images are transferred to a Macintosh IIci computer and processing is done using a commercial image processing and analysis software program, ULTIMAGE (1988). To record final images, the Macintosh screen is photographed either in black and white or color using a 35mm camera. Images included in this report are copies of photographs from the screen. Pixel coordinates within an image can be calibrated and the sample stage can be set at these coordinates to identify individual features by their X-ray emission.

The photomultiplier can be replaced by a fiber optic pickup to transmit CL to a grating spectrometer with the dispersed light incident on a intensifier and detected by a 1024 element diode array detector. Using a scanning CL image as a guide for selecting individual points, spectra from these points can be recorded using a focused electron beam. In addition, either qualitative or quantitative elemental analyses can be made allowing a correlation of chemistry with CL spectra at a series of points.

Examples of CL images and their analysis

A. Diamond. The CL of diamond is intense and the image shown in Fig. 1A shows a complex pattern of intensity variation. This image is of an inner 2 mm area of a 6 mm polished diamond plate and and was obtained by stage scanning. The diamond sample is optically featureless and is an example of extreme CL variation in a chemically simple material. The surface of the plate is perpendicular to [001] and the cubic symmetry of the CL pattern is apparent. Overall, the outer 2 mm region of the diamond shows only weak, uniform CL. The interior shows brilliant CL in a complex pattern which does not form continuous concentric bands. The boundary between the outer and interior regions, although not continuous, is distinctly brighter although not around the whole boundary. Within this boundary zone, the CL pattern is unusual in being composed of thin parallel yellow plates (Fig. 2). This CL colors were documented by returning to the bright areas recognized in the digital image and obtaining CL spectra from this bright boundary and comparing it to CL spectra from other areas. Figure 3 shows typical spectra from the diamond (peak near 470nm) as compared to the bright area (peak near 560nm). Based on the

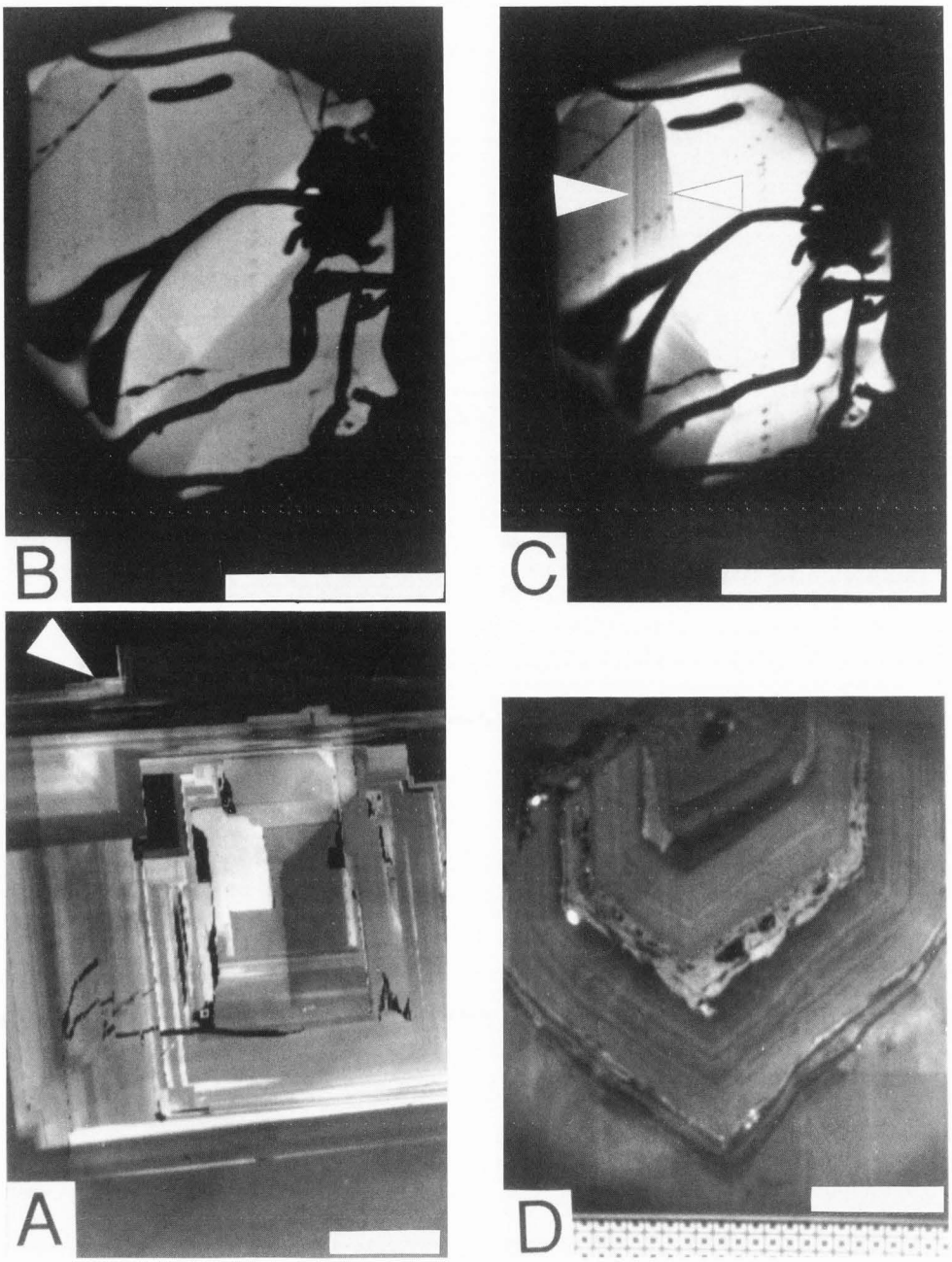

Figure 1. A) Digital CL image of interior of diamond plate. Complex CL pattern in interior contrasts with uniform CL at top and bottom of image. Arrow at upper left indicates a bright boundary between uniform and complex CL patterns. A similar area is shown in Fig. 2 at high magnification. Scale bar = 300μm. Beam conditions: 15kV, 2nA.
B) Digital CL image of interior of forsterite grain in Allende meteorite. Faint zoning pattern can be recognized. The CL emitting area is surrounded by non-luminescing forsterite. Scale bar = 200 μm. Beam conditions: 15kV, 25nA.
C) Same region as 1B but with enhanced contrast which clearly shows fine-scale parallel bands with CL contrast. A CL profile between the two arrows is shown in Fig. 4. Fine dots in line represent points analyzed using a fixed electron beam. Scale bar = 200 μm.
D) Digital CL image of growth banding in calcite crystal. Small areas with very bright CL are unidentified. Scale bar = 100 μm. Beam conditions: 15kV, 10nA.

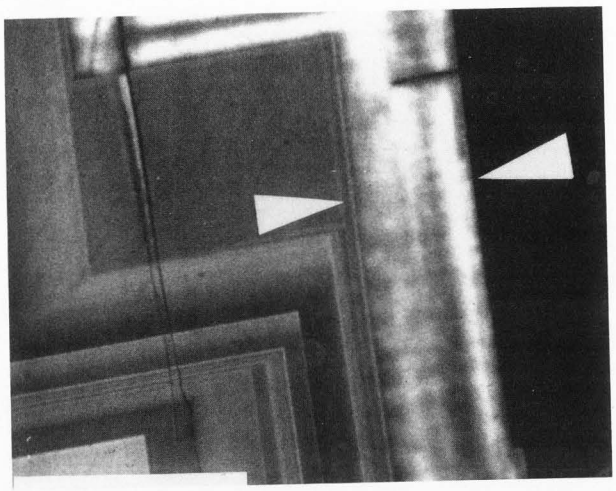

Figure 2. Scanning CL image of bright region indicated by arrow in Fig. 1A. Faint horizontal 'plates' are thought to represent giant platelets. Scale bar = 100 μm. Beam conditions: 15kV, 2nA.

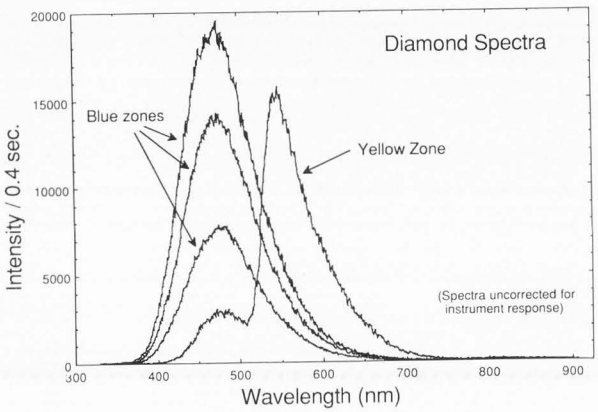

Figure 3. CL spectra from diamond of Fig. 1A. The 3 spectra labeled 'blue zones' show typical diamond spectra with a maximum intensity in the blue. In contrast, the spectra labeled 'yellow zone' is from the bright region indicated by arrow in Fig. 1A and is thought to represent emission from platelets as imaged in Fig. 2. Spectra are not corrected for instrument response. Beam conditions: 15kV, 2nA.

morphology of the plates in the yellow zone, as well as the emission spectrum labeled 'yellow' on Fig. 3, a good correspondence is seen with the previously described platelet emission at 550nm (Collins and Woods 1982). Such platelets correspond to high concentrations of nitrogen but the significance regarding formation is not certain.

B. Forsterite ($(Mg,Fe)_2SiO_4$). Forsterite is one of the most common phases within meteorites and often shows low Fe concentration. When FeO concentrations range from 0.0 to 0.5 wt.%, its brilliant CL readily distinguishes nearly pure forsterite (Mg_2SiO_4) from more Fe-rich olivine and other phases in complex meteorites (Steele, 1986a, 1986b, 1990). Luminescent forsterite is especially significant because, in contrast to most olivine, forsterite grains have an unusual minor element composition with high Al, Ti, V and Sc unlike nearly all other natural olivines and this attests to an unusual mode of formation (Steele, 1986a). In addition, isotopic analysis of oxygen for several of the forsterites has shown an enrichment of ^{16}O beyond that expected from normal processes (Weinbruch et al., 1989) and indicates that this phase grew under conditions distinct from most meteoritic material and then was incorporated into a growing meteorite body some 4.5 billion years ago (Steele, 1989).

Digital CL images of these forsterites have revealed an extremely complex textural pattern which can not be imaged with any other technique including BSE. The textures indicate a complex growth process possibly from an inhomogeneous environment followed by rapid cooling. While these textural features can be seen in scanning CL images, certain details and textures can be accentuated only by using image processing techniques. An example of the texture revealed by CL is shown in Figures 1B and 1C. A 0.5 mm size area of the interior of a polished, flat surface of a forsterite grain from the Allende meteorite is shown. While a number of intensity variations and boundaries can be seen, the enhanced digital image in Figure 1C of this same grain shows additional textural patterns barely recognizable on Fig. 1B. The CL features and a brief interpretation of forsterite in the Allende meteorite follow.

1) Only the interior of forsterite grains show CL and grains in this meteorite always show a complete rim of non-luminescing olivine with sharp boundaries between the luminescing and non-luminescing regions. While the lack of CL can be accounted for by increased FeO toward the grain margin, the sharp boundary, clearly seen in both Figs. 1B and 1C, indicates a rapid change in growth conditions with later growth under conditions allowing FeO to enter the olivine structure. One possible change includes an increased availability of oxidized Fe.

2) Numerous black (non-luminescing bands) cross the luminescing grain interior. Each represents a former fracture, now not recognizable, where the forsterite is enriched in Fe on either side of the former fracture. This indicates that the fractures were formed after grain growth but prior to the growth of the non-luminescent Fe-rich rim.

3) Fine scale concentric banding can be recognized in the enhanced image (Fig. 3C). This

banding is crystallographically controlled as it is parallel to the growth directions of the crystal recognized both by the well developed CL boundaries and also by the external morphology (not shown). The width of the individual bands as well as the relative intensity variation between bands can be directly obtained from the variation in digital intensity as shown in the line profile of Figure 4. This profile shows an oscillation period of about 5 microns and at least 8 maxima within this 40 micron traverse. Greater detail could be obtained with a finer grid increment during scanning but the resolution could not be increased below about 1 micron in the CL image due to inherent spreading of the electron beam.

4) The enhanced image of forsterite (Fig. 3C) clearly shows a bright right and dull left half but with an irregular, but approximately vertical sharp boundary. This boundary coincides with the change in direction of the fine oscillatory zoning and serves to accentuate different growth sectors of the forsterite crystal.

It must be emphasized that none of these observations are reflected in routine X-ray or BSE images and it was only with CL images that the complexity was realized. Since recognition, detailed compositional profiles have been made along traverses like that shown in Fig. 4. The bright zones in this image are characterized by high Al, Ti, and V relative to the neighboring dark zones and all three elements are highly correlated. Iron, Mn and Cr all are constant within error across these zones (Steele, 1989). This suggests, but does not prove, that the CL is due to Al, Ti, V or associated defects. The oscillatory zoning is an important observation regarding the formation as it clearly shows periodic variations in conditions during growth in contrast to steady state migration of elements to the growing crystal boundary. Since this complex zoning was recognized, many other instances have been documented and it appears to be a common phenomenon. Another important observation is that the fine scale compositional variations are retained because at the growth temperature of forsterite (1400°C), diffusion would rapidly homogenize or at least reduce the sharpness of the internal boundaries. Unfortunately the required diffusion coefficients are not known preventing calculation of temperature-time constraints.

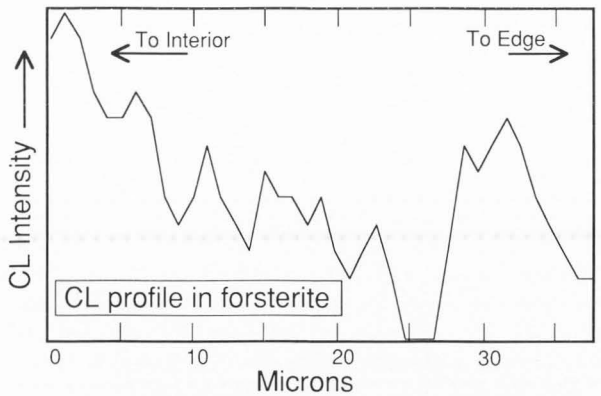

Figure 4. CL intensity variation for 40 micron profile indicated in Fig. 1C. Interior refers to central area of grain, exterior to edge of grain. The intensity maxima show regular spacing with 8 recognized peaks with a 5 μm period.

C. Carbonate zoning. (Ca, Mg)CO_3 is one of the most common terrestrial mineral phases and commonly shows spectacular CL often with complex banded textures suggesting changing conditions during growth. The CL is usually attributed to minor to trace Mn^{+2} which is in turn affected by the levels of trace to minor Fe^{+2} (Mason, 1987; Marshall, 1988). The mutual effects have been documented qualitatively but it is not certain that Mn^{+2} is the only activator and whether Fe^{+2} is the only modifier (Mason, 1987). For a large number of points where CL intensity and Fe and Mn concentrations have been measured in carbonates, the main influencing factors appear to be the Mn and Fe concentrations and the Mn/Fe ratio (Mason, 1987; Hemming et al., 1989). An important point to bear in mind is that both Mn and Fe can exist as either divalent or trivalent and concentration measurements based on microprobe data do not indicate charge state. Thus correlations between CL intensity and concentration may not always be meaningful. Fig. 1D shows a CL digital image of a 1 mm fracture-filling calcite grain from Iowa. Complex and intricate growth banding is clearly shown and Fig. 5 shows digital X-ray images of this same grain for Mg, Si, Mn and Fe. Comparison of these images shows that the brightness in the CL image does not correspond well to any of the four elements shown in Fig. 5. For Mn, the outer zones clearly have more Mn than the core but the CL in these two regions is very similar. Possibly a better correlation can be made with Mg where regions of low Mg are brightest on the CL image. These qualitative relations suggest complexities in any cause and effect relation and suggest caution should be used in interpreting the meaning of the CL in carbonates. In this case it is apparent that the CL is not a simple function of the concentration of one element as also concluded by Mason (1987). Within these images however, there are sufficient quantitative data to test models because at each point there is intensity data for Mn, Fe, Si and Mg as well as a CL intensity. Various functions of these elements and their combinations can be formulated and the digital data used among images to test possible relations. It must be kept in mind that other influencing factors in addition to these four elements are possible.

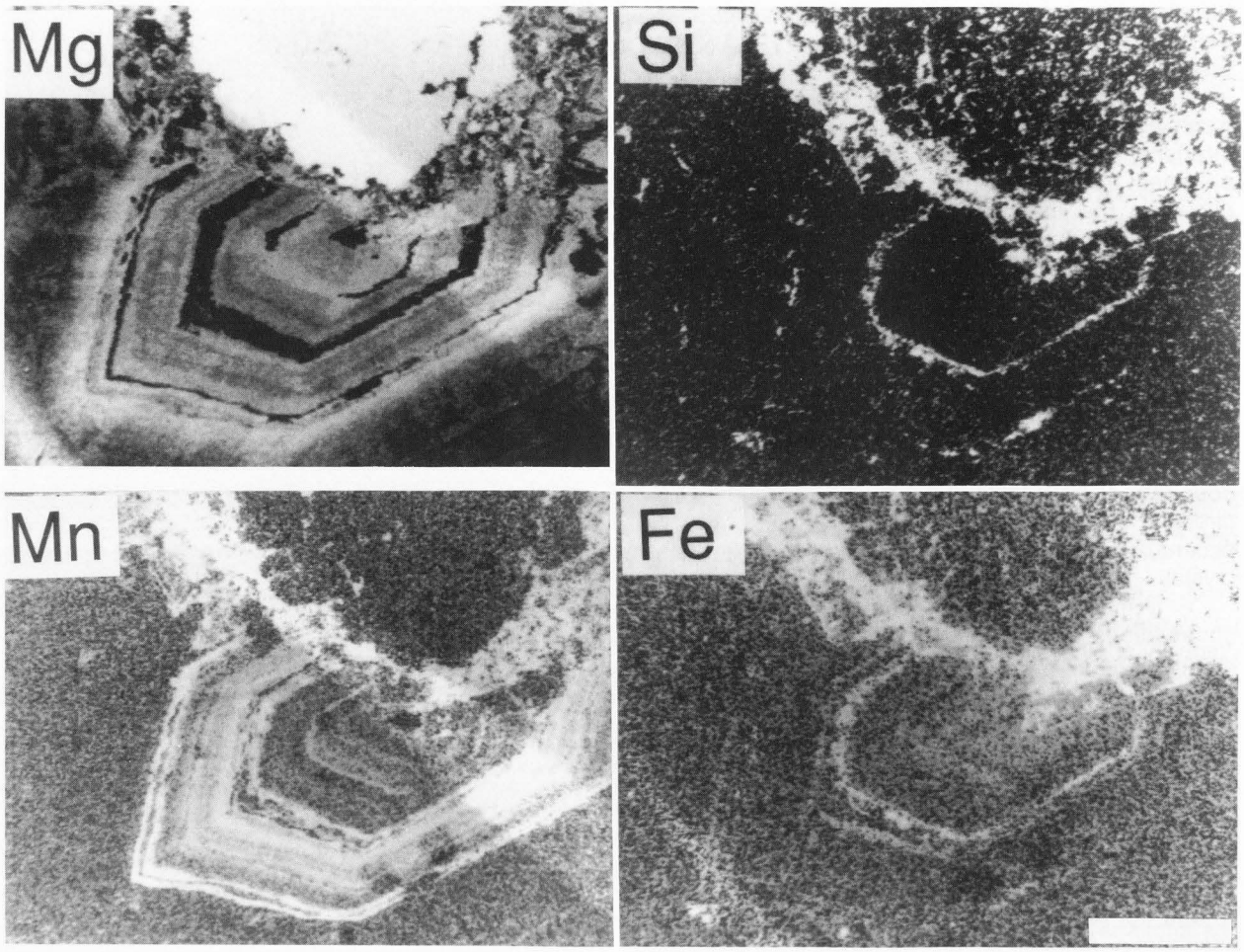

Figure 5. Digital X-ray images for Mg, Si, Mn and Fe of the same grain shown in Fig. 1D but rotated and to a slightly different scale. Comparison shows rather poor agreement between the CL intensity and the Mn concentration, the element usually considered to cause CL in calcite. On the other hand, the Mg concentration shows a inverse correlation with the CL intensity indicating a more complex relation between CL and minor element content. Scale bar = 100 μm.

D. Complex intergrowths. The phases described in above sections A-C are relatively simple but more often than not, natural systems provide examples of intergrown phases which may or may not show CL. One example is shown in Fig. 6 which is a digital CL image of a portion of a large crystal of melilite. The central portion is brightly luminescent and is mainly $Ca_2Al_2SiO_7$ while the rim which is weakly luminescent is enriched in $Ca_2MgSi_2O_7$. Within this crystal many grains of spinel, $MgAl_2O_4$, are included. This is best seen on the BSE image at the bottom of Fig. 6 where each inclusion appears as a dark, equidimensional grain. Other features which can readily be recognized on the CL image include dark, elliptical shaped areas in the CL image which are former analysis areas from an ion microprobe beam and rows of fine dark dots which represent electron probe damage spots. While the spinels are all nominally the same composition, their CL shows a wide range. Most are very bright and appear white due to overexposure in the CL image. Others, however are much darker and appear as groups of grains as indicated by a and b on Fig. 6. For the area labeled a, the spinel grains show almost no CL but are surrounded by grains showing bright CL. In area b (Fig. 6) the spinels show intermediate CL, are clustered, and are partly surrounded by spinels showing bright CL.

This example illustrates the sensitivity of CL in showing fine distinctions between grains which are nominally the same composition and which appear to have grown in close proximity. One possible interpretation is that some of these grains did not grow

in place but were rather inherited from a pre-existing mineral assemblage and have retained that chemical signature. Although other explanations are possible, this is used as a complex example where CL provides additional information to constrain interpretation.

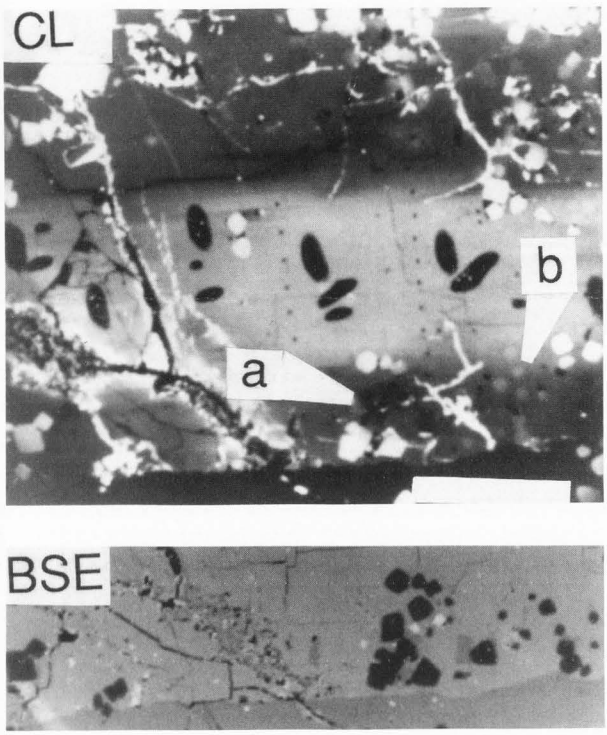

Figure 6. Cathodoluminescence (CL) and backscattered electron (BSE) images of zoned melilite grain in the Allende meteorite. The BSE image repesents only the bottom portion of the CL image. The CL image shows a broad bright horizontal band which is the core of the melilite ($CaAl_2SiO_7$). The composition becomes enriched in $CaMgSi_2O_7$ toward top and bottom as shown by darker CL. Included within the melilite are many small spinel ($MgAl_2O_4$) grains best seen as dark areas on the BSE image. Careful examination shows that these spinel grains show a range of CL brightness. Most are bright, but clusters of spinels marked by (b) are gray while another cluster (a) shows no CL. The range in CL of spinels implies different environments of formation although now the grains are intimately mixed, but grouped. Scale bar = 100μm. Beam conditions: 15kV, 25nA.

Summary

Digital acquisition of cathodoluminescence images can be routinely accomplished using electron beam instruments and these images provide an additional perspective for interpretation of textures and compositional variations in simple and complex materials. In some cases, the CL images point to inhomogeneities which can not be recognized by other techniques. The CL images can seldom be interpreted by themselves but rather complement conventional compositional maps as represented by BSE and X-ray images. Additional refinements can be made in the technique including image processing to enhance specific features, multiple correlation between images to access cause and effect in the CL images, and collection of specific wavelength ranges of the CL spectrum by placing the photomultiplier after a dispersing optical element to give a wavelength specific image albeit with reduced intensity.

Acknowledgments

Financial support was derived from NASA NAG 9-47 and instrumental support through NSF EAR-8415791 and NSF EAR-8608299.

References

Collins AT, Woods GS (1982): Cathodoluminescence from 'giant' platelets, and of the 2.526 eV vibronic system, in type Ia diamonds. *Phil Mag* 45, 385-397.

Hemming NG, Meyers WJ, Grams JC (1989): Cathodoluminescence in diagenetic calcites: the roles of Fe and Mn as deduced from electron probe and spectrophotometric measurements. *J. Sedimentary Petrology* 59, 404-411.

Marshall DL (1988): *Cathodoluminescence of geological materials*, Unwin Hyman, Boston 146 pages.

Mason RA (1987): Ion microprobe analysis of trace elements in calcite with an application to the cathodoluminescence zonation of limestone cements from the lower carboniferous of south Wales, U.K. *Chemical Geology* 64, 209-224.

Steele IM (1986a): Compositions and textures of relic forsterite in carbonaceous and unequilibrated ordinary chondrites. *Geochim. Cosmochim. Acta* 50, 1379-1396.

Steele IM (1986b): Cathodoluminescence and minor elements in forsterite from extraterrestrial samples. *Am. Mineral.* 71, 966-970.

Steele IM (1989): Compositions of isolated forsterites in Ornans (C3O). *Geochim. Cosmochim. Acta* 53, 2069-2080.

Steele IM (1990): Mineralogy of meteorites revealed by cathodoluminescence. In *Spectroscopic Characterization of Minerals and Their Surfaces* (Coyne LM, McKeever SWS, Blake DF, Eds.) American Chemical Society, Washington, DC 150 - 164.

ULTIMAGE: Image processing and analysis software for the Apple Macintosh II. Graftec, France. Distributed in U.S. by GTFS, Inc., 2455 Bennett Valley

Rd., #100C, Santa Rosa, CA 95404.

Weinbruch S, Zinner EK, Steele IM, El Goresy A, Palme H (1989): Oxygen-isotopic compositions of Allende olivines (abstract). *Proc 52nd Meteoritical Society*, 262.

Discussion with Reviewers

G. Remond: Comparisons between CL emissions and impurity analyses indicate that Mn is probably not the only activator of the CL emission of calcite crystals. Are CL spectra available to indicate if the CL contrast shown on the panchromatic CL image of the calcite crystal resulted from only a change in CL intensity or from a change in the CL emission spectrum at different locations on the specimen surface?

Author: For the example given here, spectra are not available. However, as described in the equipment section, I do have a grating spectrometer, image intensifier and diode array detector and a worthwhile experiment would be to collect a series of spectra which can be easily correlated with the position within the image using the stage precision of $\pm 1 \mu m$. For each of these points, an analysis can also be obtained to correlate the CL spectrum with chemical variation at least for elements detectable with the electron probe.